Definition of an uni-axial equivalent testing procedure for a multi-axial random fatigue loading assessment

Luca Campello

CSMA 2024
16ème Colloque National en Calcul des Structures
13-17 Mai 2024, Presqu'île de Giens (Var)

Definition of an uni-axial equivalent testing procedure for a multi-axial random fatigue loading assessment

L. Campello[1 2], R. Sesana[2], R. Serra[1] and C. Delprete[1]

[1] *LaMé, INSA Centre-Val de Loire, France, {luca.campello, roger.serra}@insa-cvl.fr*
[2] *DIMEAS, Politecnico di Torino, Italy,{ luca.campello, raffaella.sesana, cristiana.delprete} @polito.it*

Résumé — Many mechanical components experience a multi-axial random loading in their service life, which could lead a fatigue failure. Nowadays, to overcome the lack of appropriate testing setup, the assessment of structural integrity of the components is performed by several testing procedures like loading alongside different axis in sequential manner, specific test setup or particularly geometry of the specimens. The objective of this research is to develop an equivalent single-axis random excitation system estimation model to predict the life of multi-axial loaded random fatigue system.
Mots clés — Multi-axial random loading, Single-axis random loading, Dynamic Numerical Simulation, Experimental Validation.

1 Introduction

Mechanical components are often excited by random loadings exposing them to a local random stress that could be uni-axial or multi-axial stress. If those tyme varying loads endure for long time, they could lead to a fatigue failure caused by damage accumulation. So vibration environment test play an important role in order to carry out structural durability assessment [8, 10].

If the local stress is uni-axial, to compute the fatigue damage and the residual fatigue life, the approach consists in using counting method of time signal and Palmgreen-Miner laws. The analysis can be conducted in frequency domain, relying on the spectral damage methods (i.e., Dirlik, Tovo-Benasciutti,...) [11].

If, the local stress is multi-axial, the analysis results to be more complex, and it requires the use of multi-axial life and damage estimation criteria. In literature, several models to estimate the damage and the fatigue life for multi-axial random loads are presented, based on different approach as critical plane, stress invariant or equivalent Von Mises stress in frequency domain [2].

Despite the improvement in theoretical and numerical analysis, creating test specification to evaluate the fatigue damage produced by vibration in the real environment remain one most difficult task. The life cycle prediction under multi-axial dynamic loading turned out to be very complex and more difficult than under uni-axial loading. The current capability to perform multi-axial fatigue tests is adversely affected by the high cost of development of such testing methods and the lack of existing equipment to conduct the necessary tests [7].

However, due to this limitation, one of the solution, proposed by military and commercial standards is to excite different axis of the structure in a sequential manner. Some researchers [13, 14, 6, 12] has pointed out that, even if this technique is widely used, it does not excite a stress state that are likely to exist in a true operational environment with multi-axis input, leading to a failure mode being missed or a overestimation of the failure times.

Otherwise, a layout with two independent uni-axial shakers, one mounted to an arm parallel to the specimen and the second to an arms perpendicular to the specimen, can help to achieve a coupled or uncoupled bending-torsion loading [9]. Of course, this layout system require two uni-axial testing system. This system yields a pure bending loading when only the arm parallel to specimen axis is excited. Instead, if the excitation is only imposed by the other shaker (arm perpendicular to the specimen), the specimen is subjected to torsion loading, without bending.

Another layout [15] could be a special holder structure designed to control independently bending and torsion loading. It was designed to decoupled the bending and torsion, but it needs a tri-axis shaker.

In some other cases, particular geometries of specimen are adopted to have a multi-axial state of stress, like a trapezoidal plate [5], where a in-phase bi-axial bending deformation is obtained, or a Y-shaped specimen with two tipped masses that develop a multi axial stress when subjected to a vertical base excitation [3].

The purpose of the present paper is to present an experimental single axis excitation setup able to develop a multi-axial stress state condition. This condition is obtained by adding a T-shaped mass at the free end of a cantilever beam to create a bending-torsion coupled loading. This paper is in the framework of a research whose aim is develop single axis random fatigue life estimation model able to estimate the life of multi-axis loaded random fatigue systems.

2 Theoretical Background

Let's consider a cantilever beam, with a mass per length ρ, under based excitation with a mounted mass M_t, with a mass moment I_t, on the free end as in Figure 1. Let's indicate $\nu(x,t)$ as transverse displacement of the neutral axis (at point x and time t) due to bending, $\ddot{w}(t)$ as the base motion's acceleration and $\ddot{z}(x,t)$ the beam's neutral axis absolute acceleration. Let's introduce $\ddot{\nu}(x,t)$ as the beam's neutral axis transverse relative acceleration, computed as

$$\ddot{\nu}(x,t) = \ddot{z}(x,t) - \ddot{w}(t) \tag{1}$$

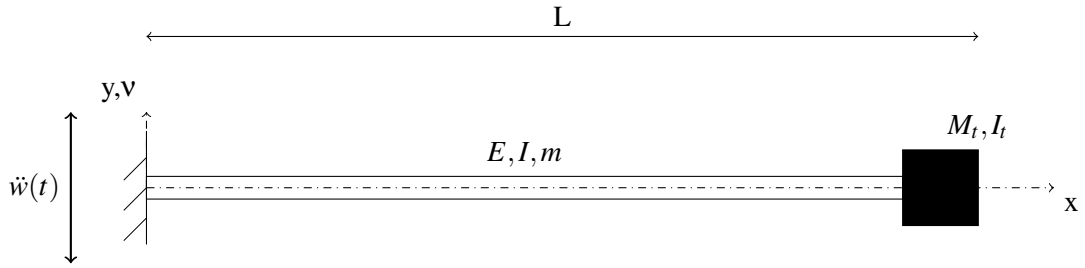

FIGURE 1 – Cantilever beam with a tip mass at the end subjected to base excitation

The governing equation of the motion can be expressed as [4]

$$EI\,\frac{\partial^4 \nu}{\partial x^4} + m\frac{\partial^2 \nu}{\partial x^2} = -m\frac{\partial^2 w}{\partial t^2} \tag{2}$$

where EI is the bending stiffness and m is the mass per unit length of the beam. The boundary condition of the system are as follow

$$\nu(0,t) = 0 \qquad \left[\frac{\partial \nu(x,t)}{\partial x}\right]_{x=0} = 0 \tag{3}$$

$$\left[EI\,\frac{\partial^2 \nu(x,t)}{\partial x^2} + I_t\frac{\partial^3 \nu(x,t)}{\partial x^2}\right]_{x=L} = 0, \quad \left[EI\,\frac{\partial^3 \nu(x,t)}{\partial x^3} + M_t\frac{\partial^2 \nu(x,t)}{\partial t^2}\right]_{x=L} = 0 \tag{4}$$

Using the method of separation of variables, the *characteristic equation* of the differential is obtained as [**?**] :

$$\begin{aligned} &1+\cos\lambda\,\cosh\lambda+\lambda\frac{M_t}{mL}(\cos\lambda\,\sinh\lambda-\sin\lambda\,\cosh\lambda)-\frac{\lambda^3 I_t}{mL^3}(\cosh\lambda\,\sin\lambda+\sinh\lambda\,\cos\lambda)+\\ &\frac{\lambda^4 M_t I_t}{m^2 L^4}(1-\cos\lambda\,\cosh\lambda)=0 \end{aligned} \tag{5}$$

The solution of the equation are the eigenvalues of the system, denoted as λ and the *bending undamped natural frequencies* of the free oscillations for the r_{th} vibration mode is obtained as

$$\omega_r = \lambda_r^2 \sqrt{\frac{EI}{mL^4}} \tag{6}$$

3 Numerical Simulation

The purpose of the simulation is to conduct a numerical modal analysis to obtain natural frequencies of the specimen, to compute the simulated frequency response function (FRF) and to evaluate the stress components on the specimen. The software used is Altair HyperWorks. All the materials of the system were modellised as isotropic. The numerical model of the system is depicted in Figure 2. The total number of elements are 25134 : 25047 are hexaedra 8 points, 87 are pentahedra 6 points. Across the thickness, there are five elements. The average elements size change based on the components of the system. For the acceleromenters, it is 2mm, for the support, it is 3 mm and for the specimen it changes according the position : the size around the notches is 0.5 mm in order to obtain a more precise value of stress, and in the rest of the specimen the average size is 1.5 mm. 850 elements were constrained in all the axis (X, Y and Z) to simulate the clamping system of the shaker.

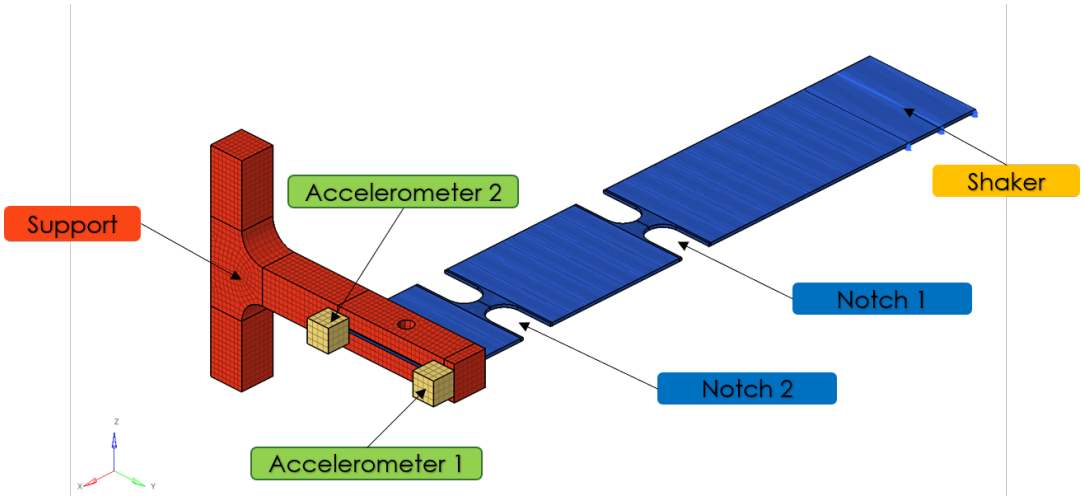

FIGURE 2 – Numerical Model of the system

3.1 Modal Analysis

As regards the modal analysis, the first three natural frequencies (Table 1) have been compute : the first mode consist in a bending mode, the second mode is a torsional mode while the third is again a bending mode.

TABLE 1 – Numerical natural frequency

	$1^{st}mode$	$2^{nd}mode$	$3^{rd}mode$
Numerical Frequencies $[Hz]$	11.3	40	76
Partecipation Factors	0.27	0.042	0.15
Mode	Bending	Torsion	Bending

In Figure 3 the first three natural modes are illustrated. It is worth noting that, in the torsional mode, because of the asymmetrical geometry of the T-shaped component respect to X axis, the center of rotation is outside the longitudinal axis of the specimen. Therefore all the points of the free edge of the specimen rotate around this point and, as demonstrated by the kinematics's laws, the accelerometer 1 measured an higher acceleration than accelerometer 2

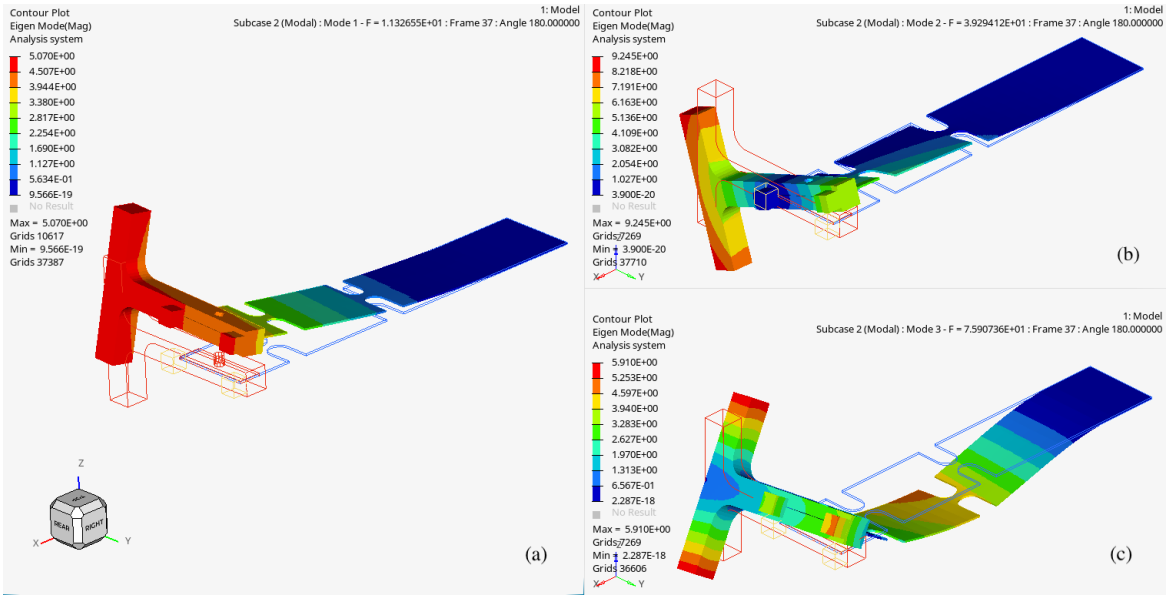

FIGURE 3 – Modal displacement of natural modes :(a) I mode, (b) II mode, (c) III mode

4 Experimental validation of the numerical model

4.1 Testing setup

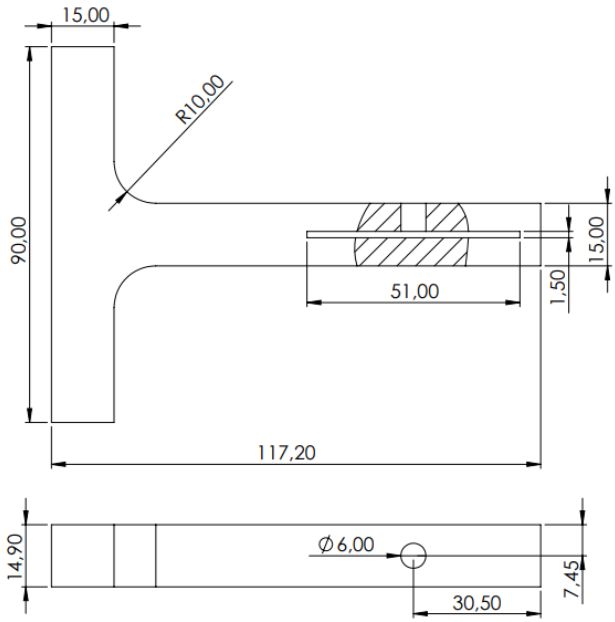

FIGURE 4 – T-shaped Support

The testing setup consisted on a metallic sheet made with two notches, with a thickness of 1.2 mm in one of the two edges a T-shaped support was fixed ((Figure 4). The material and physical properties of each components are shown in Table 2.

4.2 Experimental Modal Analysis

The first experimental validation was Experimental Modal Analysis (EMA). The testing setup was clamped as in Figure 6. The test consisted in hitting the specimen with an impact hammer in 31 different points to extract the natural frequencies and natural modes. The software used for the analysis was Dewesoft. The performance of the numerical results was evaluated by applying a percent relative error

TABLE 2 – Mechanical properties of setup components

	Specimen	Support	Accelerometer
Material	AISI 304	PLA	Titanium
Mass $[g]$	111.5	20.2	4.8
Density $[kg/m^3]$	7965	478	4800
Young's modulus (E)$[GPa]$	185	1.3	120

E, defined as

$$E = \frac{f_{exp} - f_{num}}{f_{exp}} \tag{7}$$

where f_{exp} is the experimental frequency and f_{num} is the numerical frequency. In Table 3 a comparison between experimental and numerical natural frequencies show satisfactory results considering that maximum values of relative error is 5%. Indeed, from Figure 5 experimental modal deformation are reported. It is to be noted the correspondence between the experimental modes shapes and the numerical ones for the second and third modes.

TABLE 3 – Comparison between experimental and numerical natural frequencies

Frequencies	Experimental[Hz]	Numerical [Hz]	Relative Error (%)
f_1	11,2	11,3	1
f_2	42	40	5
f_3	72	76	4

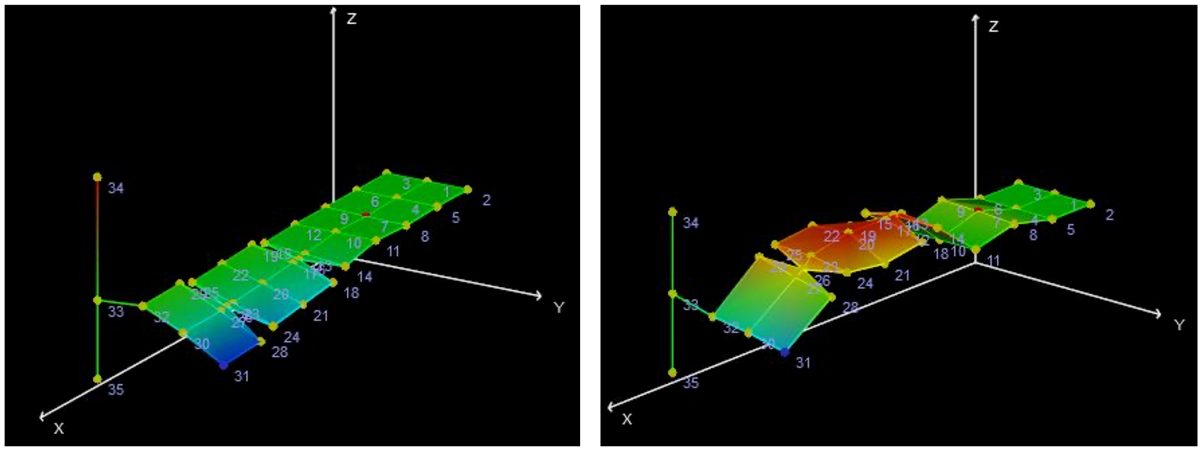

FIGURE 5 – Experimental mode shapes

4.3 Accelerated Test

The testing procedure (Figure 6) consisted in clamping the specimen on a uni-axial shaker. Two accelerometers were placed to acquire the acceleration of the two edges of the specimen's free end. Because of the shaker has a closed-loop control system, a third accelerometer is placed at the center of the clamping system as a feedback for the input acceleration.

By evaluating the natural frequencies, natural modes and participation factors, from numerical analysis, the frequency range from 20Hz to 110 Hz, that include the second and the third natural mode, was recognize as the most suitable to perform the test. The level of acceleration was 0.25g. The frequency rate was 5 Hz/min. Two different specimens have been used, called A1 and A2, and for each specimen 4 repetitions have been carried out.

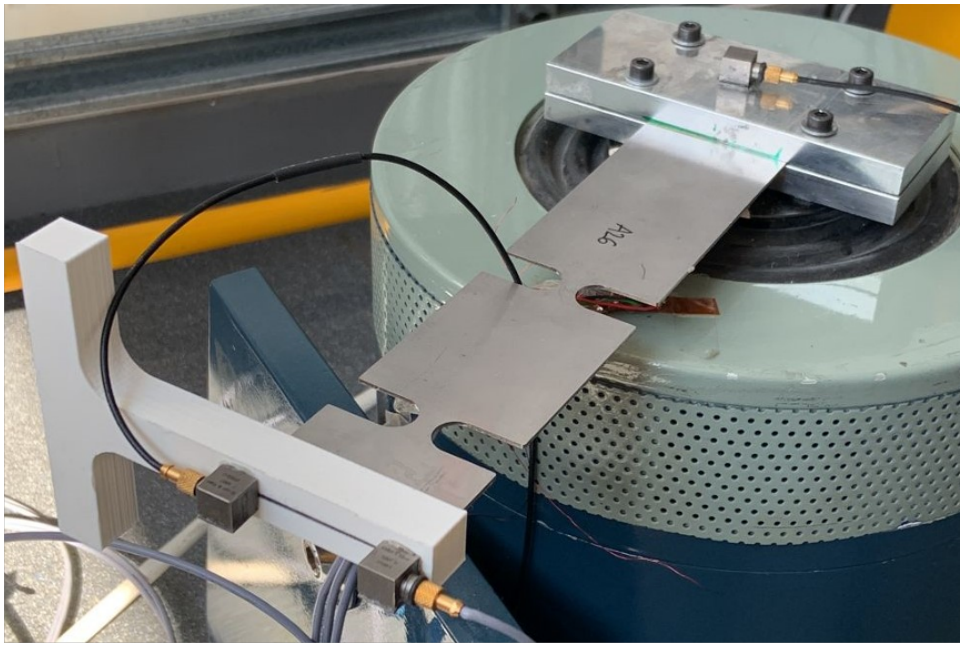

FIGURE 6 – Experimental Setup

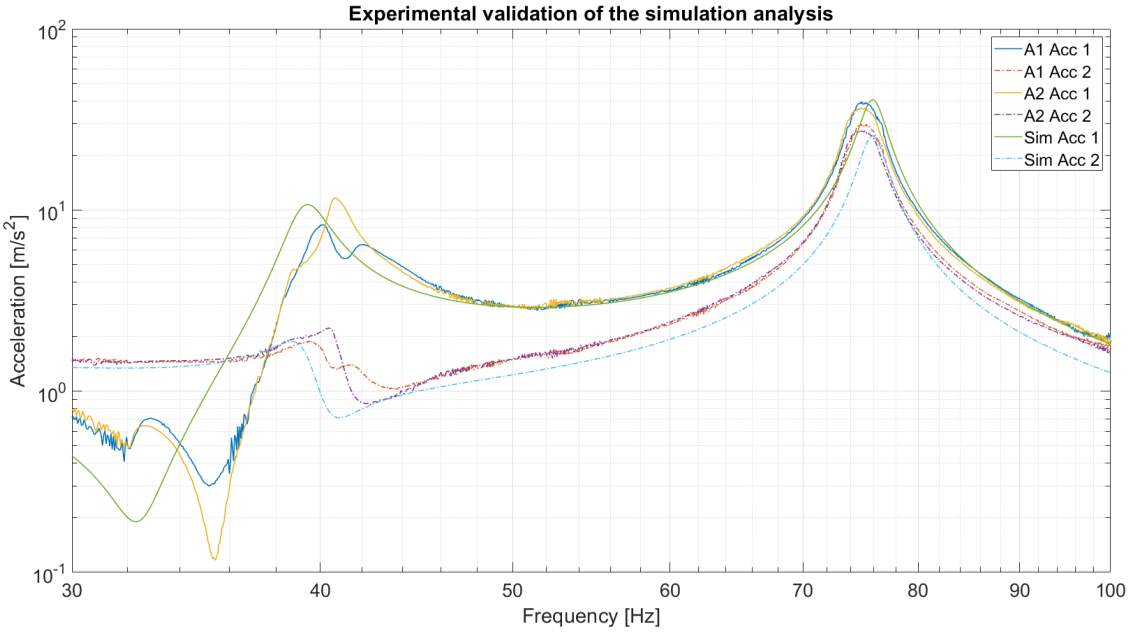

FIGURE 7 – Comparison between experimental and numerical setup

In Figure 7, a comparison between the simulation and experimental frequency response function is illustrated. The correct damping values 2ζ, reported on Table 4 on numerical model have been obtained by iteration as long as the numerical plot corresponded to the experimental ones.

TABLE 4 – Numerical Damping values

f	2ζ
f_2	0.05
f_3	0.04

As shown in the plot, around the frequency of 40Hz, there is a remarkable difference in term of acceleration between the two accelerometers. The accelerometer 1 (Figure 2) measured an higher acce-

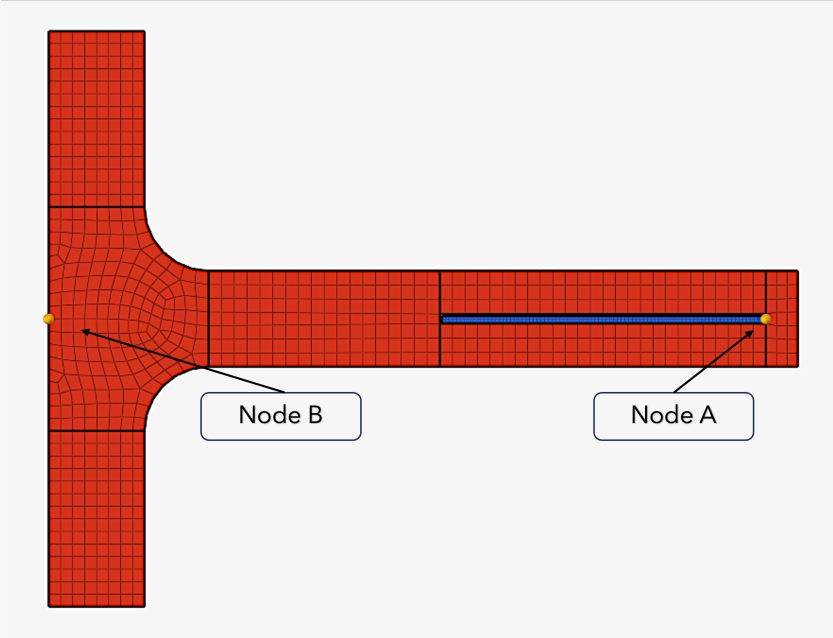

FIGURE 8 – Point A and B

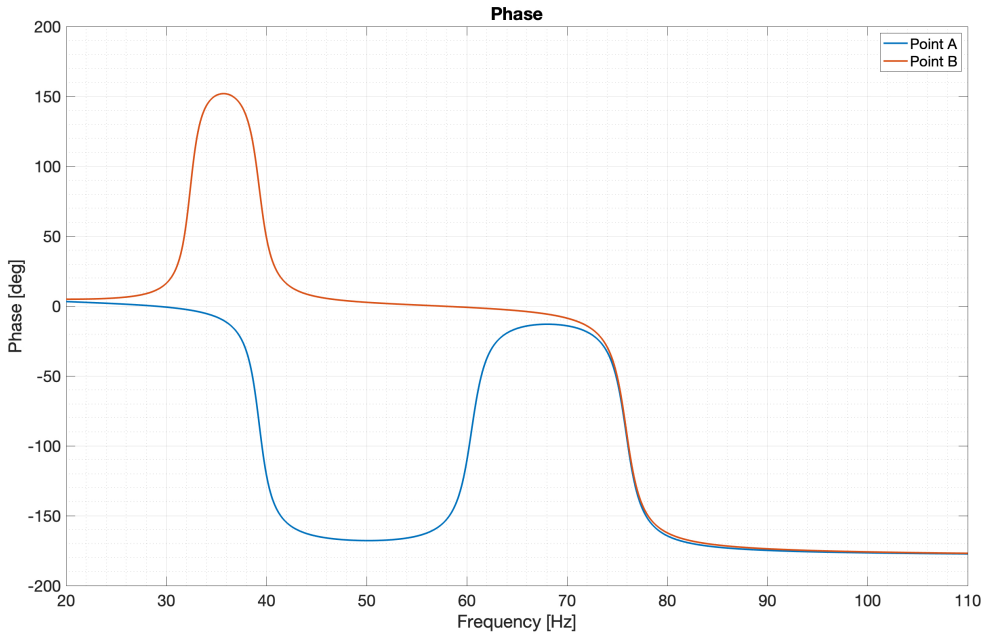

FIGURE 9 – Phase of Point A and B

leration than accelerometer 2, meaning that the specimen experienced a torsional deformation. A second validation of the torsional mode come from the phase plot (Figure 9) of two points (Figure 8). Around 40 Hz the point A and point B show phase of opposite sign and therefore a rotation along specimen longitudinal axis occurred. It is worth pointing out that the torsional deformation is a relevant effect of the T-shaped component on the dynamic behavior of the specimen. Indeed, without it, the specimen has only bending deformation [1].

Comparing the natural bending frequency of the system with analytical bending frequencies of the Bernoulli-Euler beam proposed in Figure 1 (Table 5) with Eq. 6 it can be stated that the first bending natural frequencies of the two models are very close, but at higher frequencies the difference increases. This is because the Bernoulli-Euler beam model considers a symmetric system with only bending modes. In this case, the system is asymmetric and therefore every bending mode is affected by a contribution of torsional deformation.

TABLE 5 – Comparison of bending natural frequency

f	Analytical Frequencies [Hz]	Numerical Frequencies[Hz]	Δ	Relative Error [%]
f_1	11.3	11.32	0.02	0.17
f_2	75.3	75.9	0.6	0.8
f_3	209.2	185.5	23.7	11.3
f_4	387	403.3	16.3	4.2
f_5	613.5	587	26.5	4.3

5 Conclusion

In this paper, a new test setup for random fatigue testing of flat metallic specimen with unidirectional exciter and his corresponding numerical model was described. A dynamic numerical evaluation of the system was performed and compared with experimental results. the results of the comparison show that the simulations were in good agreement with the experimental tests. A future step of the research will be the fatigue evaluation of the system loaded by random vibration, to discover which modes, torsion or bending, contribute mostly to the fatigue failure of the specimen, and how the failure modes will looks like.

Références

[1] L. Campello, R. Serra, R. Sesana, C. Delprete. *Fatigue Damage Estimation from Random Vibration Testing : Application to a notched specimen*, 15éme Colloque National en Calcul des Structures, 2021

[2] A. Carpinteri, A. Spagnoli, S. Vantadori. *A review of multiaxial fatigue criteria for random variable amplitude loads*, Fatigue & Fracture of Engineering Materials & Structures, 1007-1036, 2017

[3] M. Česnik and J. Slavič and M. Boltežar. *Uninterrupted and accelerated vibrational fatigue testing with simultaneous monitoring of the natural frequency and damping*, Journal of Sound and Vibration, 5370-5382, 2012

[4] A. Erturk and D. J. Inman. *Piezoelectric Energy Harvesting*, John Wiley & Sons, 2011.

[5] T.J. George, J. Seidt, M.H. Shen, T. Nicholas, C.J. Cross. *Development of a novel vibration-based fatigue testing methodology*, Int. J. Fatigue, 477 - 486, 2006

[6] M. French, and R. Handy, H.L. Cooper. *Comparison of simultaneous and sequential single axis durability testing*, Experimental Techniques, 32-37, 2006.

[7] E. Habtour, W. Connon, M. F. Pohland, S. C. Stanton, M. Paulus, A. Dasgupta. *Review of the response and Damage of linear and Nonlinear System under Multiaxial Vibration*, Shock and Vibration, 2014.

[8] G. He, H. Chen, X. He. *Fatigue behavior and influence factor analysis of the structure subject to multi-axial random loading*, Journal of Vibroengineering, 3620-3634, 2015.

[9] T. Lagoda, E. Macha, A. Nieslony. *Fatigue life calculation by means of the cycle counting and spectral methods under multiaxial random loading*, Fatigue & Fracture of Engineering Materials & Structures, 409-420, 2005

[10] J.E. Marques, D. Benasciutti, A. Nieslony, J. Slavič. *An Overview of Fatigue Testing Systems for Metals under Uniaxial and Multiaxial Random Loadings*, Metals, 2021

[11] M. Mršnik, J. Slavič, M. Boltežar. *Frequency-domain methods for a vibration-fatigue-life estimation - Application to real data*, International Journal of Fatigue, 2012.

[12] B. Owens, G. Tipton and M. McDowell. *6 Degree of Freedom Shock and Vibration : Testing ans Analysis*, Analytical Structural Dynamics Department Sandia National Laboratories, 2016

[13] W. Whiteman, M. Berman. *Fatigue Failure Results for Multi-Axial versus Uniaxial Stress Screen Vibration Testing*, Shock and Vibration, 319-328, 2002.

[14] W. Whiteman, M. Berman. *Inadequacies in uniaxial stress screen vibration testing*, Journal of the Institute of the Environmental Sciences and Technology, 20-23, 2001

[15] D. Zanellati, D. Benasciutti, R. Tovo. *An innovative system for uncoupled bending/torsion tests by tri-axis shaker : Numerical simulations and experimental results*. MATEC Web Conf.,1-7, 2018,